PHYSICAL REVIEW A VOLUME 45, NUMBER 5 1 MARCH 1992

Detection of ultrafast molecular-excited-state dynamics with time- and frequency-resolved pump-probe spectroscopy

Gerhard Stock and Wolfgang Domcke
Institut für Physikalische und Theoretische Chemie, Technische Universität München, D-8046 Garching, Germany

(Received 17 June 1991; revised manuscript received 4 November 1991)

A unified theoretical description of various forms of time- and frequency-resolved stimulated-emission pump-probe (PP) spectroscopy of molecules is outlined. The expressions for the integrated and the dispersed PP signal are derived in the limit of an optically thin medium. In the limit of ultrashort pulses, the connection between the PP signals and the appropriate time-dependent observables of the molecular system are established. The PP signals obtained with probe pulses of finite duration are expressed in terms of the simpler quantities pertaining to the ultrashort limit. The apparent paradox that it seems possible to achieve simultaneously high time and frequency resolution is discussed. It is shown that the dispersed PP spectrum carries information on electronic population dynamics, coherent excited-state vibrational motion, as well as electronic dephasing processes. It may thus be difficult to interpret in general. The integrated PP signal, on the other hand, possesses a particularly simple interpretation in the limit of ultrashort pulses: It directly reflects the electronic population dynamics of dipole-allowed excited states. The general conclusions are illustrated by computational results for a model system representing multidimensional vibrational motion and ultrafast internal conversion in excited singlet states of pyrazine.

PACS number(s): 33.80.−b, 31.70.Hq, 42.65.Re

I. INTRODUCTION

With the availability of optical and uv laser pulses with durations of the order of 10 fs [1], time-resolved pump-probe (PP) spectroscopy has become an important tool in the investigation of ultrafast molecular dynamics [2]. Femtosecond PP techniques are now extensively applied to investigate ultrafast processes in biological systems [3], the excited-state dynamics of dye molecules in solution [4–6], the relaxation of coherent transients in semiconductors [7,8], and the photodissociation dynamics of simple diatomic and triatomic systems in the gas phase [9,10].

All these experiments share the general idea that the pump pulse prepares a nonstationary state, which is interrogated by the time-delayed probe pulse. The probing of the excited-state dynamics is achieved either by monitoring the probe-pulse transmission (transient absorption) [11], by excited-state absorption with detection of fluorescence or photofragments [9,12,13], or by pulsed ionization with ion or photoelectron detection [14–17]. Depending on the probe mechanism and on laser-pulse properties, the observed signal may reflect different aspects of the dynamics of the material system. This indicates that the interpretation of time-resolved PP experiments in terms of microscopic dynamics requires a careful theoretical analysis.

There is a rapidly increasing amount of theoretical work that considers the possibility of real-time monitoring of ultrafast molecular dynamics with various probe mechanisms, including excited-state absorption [10,18], ionization [19,20], stimulated emission [21–27], and stimulated impulsive Raman scattering [26,28–31]. In the latter two cases several methods of photon detection have been considered, namely, frequency-integrated [21,22,27–31], dispersed [23–27], and polarization-sensitive [5] detection of the probe-induced emission field. A closely related problem is time-resolved fluorescence spectroscopy [32–34]. The time-dependent response of the material system, i.e., the ultrafast system dynamics to be observed, usually enters the formulation through the probe-induced third-order polarization $P^{(3)}(t)$, which has to be evaluated for an appropriate model system. The system response has been taken into account by classical models [10,35–37], one-dimensional quantum wave-packet calculations [18,25,38,39], few-level density-matrix models with phenomenologically or stochastically introduced dephasing [22–31,40], or by time-dependent quantum-mechanical multimode calculations on coupled electronic surfaces [41].

In this work we outline the theory of time- and frequency-resolved stimulated-emission experiments on molecular systems, with emphasis on the limit of ultrashort pulses. The theoretical expressions for the integrated as well as the dispersed emission spectrum are derived by solving the wave equation for the probe field in the limit of an optically thin medium. We wish to clarify, in particular, the relationship between the PP signals and appropriate observables of the time-dependent intramolecular dynamics. It will be seen that the integral and the dispersed signals elucidate different aspects of the molecular dynamics, depending on the probe-pulse duration and the coherence decay time of the probe-induced polarization. The integrated PP signal obtained with sufficiently short pulses reflects most directly the electronic population dynamics in excited states. The differential PP spectrum obtained with an ultrashort probe pulse carries additional information on coherent vibrational motion and electronic dephasing.

The general theoretical considerations will be illustrated by computational results for a simple but nontrivial model system representing multidimensional vibrational motion and ultrafast internal conversion in excited singlet states of pyrazine [42]. The example demonstrates that time- and frequency-resolved PP spectroscopy has the potential to reveal rich information on the ultrafast vibronic and vibrational dynamics in polyatomic molecules.

II. PUMP-PROBE SIGNALS

In a typical time-resolved stimulated-emission PP experiment the first (pump) pulse prepares a nonstationary vibrational state on an excited electronic potential-energy surface, which is interrogated after a delay time Δt by the second (probe) pulse through stimulated emission into the electronic ground state. As usual in the description of stimulated processes, the radiation field is treated classically. Assuming that both pulses propagate collinearly in z direction, the total electric field is written as

$$\mathbf{E}(z,t)=\sum_{i=1,2}[\varepsilon_i E_i(z,t)+\text{c.c.}]\ , \tag{1a}$$

$$E_i(z,t)=\varepsilon_i(z,t)e^{i(kz-\omega_i t)}\ , \tag{1b}$$

where ω_1, ω_2 are the laser frequencies, ε_1, ε_2 the polarization vectors, k is the z component of the wave vector, and $\varepsilon_1(z,t)$, $\varepsilon_2(z,t)$ denote the pulse envelope functions, centered at $t=0$ and $t=\Delta t$, respectively.

The experimental PP signal is usually defined as the difference between the transmission of the probe pulse with and without the preparation of the sample by the pump pulse [6,7,10]. We therefore have to consider the propagation of the probe pulse in the nonlinearly polarized medium. In the slowly varying envelope approximation, the wave equation for the probe pulse reads [43]

$$\left[\frac{\partial}{\partial z}+\frac{1}{v}\frac{\partial}{\partial t}\right]\varepsilon_2(z,t)=\frac{2\pi i\omega_2}{nc}p^{(3)}(z,t)\ , \tag{2}$$

where $n=v/c$ is the refractive index of the medium and $p^{(3)}(z,t)$ is the envelope function of the nonlinear polarization. It has to be kept in mind that the slowly varying envelope approximation may approach the limits of its validity in the case of femtosecond pulses with optical frequencies. In front of the sample ($z=0$) the incident field is given by

$$\varepsilon_2(z=0,t)=\varepsilon_2(t)\ . \tag{3}$$

We restrict the discussion to Fourier-limited laser pulses. In the numerical calculations below, Gaussian pulse envelopes are assumed.

As the nonlinear polarization $p^{(3)}(z,t)$ is itself a function of the local probe field $\varepsilon_2(z,t)$ in the sample [cf. Eq. (13)], the coupled field-material equations have to be solved self-consistently [44]. However, if we assume an optically thin sample, the incident field $\varepsilon_2(t)$ that induces the polarization passes, by definition, through the medium unchanged. In this case we may neglect the time derivative in (2) and calculate the polarization using only the incident field. We thus obtain for the field at the end of the sample ($z=l$) [5,10]

$$\varepsilon_2(l,t)=\varepsilon_2(t)+\frac{2\pi i\omega_2 l}{nc}p^{(3)}(t)\ . \tag{4}$$

Within the approximation of an optically thin medium, the total electric field is thus simply given by the sum of the incident field and the material response field, i.e., the probe-induced polarization $p^{(3)}(t)$.

The integrated pump-probe (IPP) signal is defined as the (time-integrated) intensity of the total emitted field $\varepsilon_2(l,t)$ minus the intensity of the incident field $\varepsilon_2(t)$

$$\begin{aligned}I(\Delta t)&=\int_{-\infty}^{\infty}dt[|\varepsilon_2(l,t)|^2-|\varepsilon_2(t)|^2]\\&=2\,\mathrm{Im}\omega_2\int_{-\infty}^{\infty}dt\,\varepsilon_2(t)p^{(3)*}(t)\ ,\end{aligned} \tag{5}$$

where, for convenience, a prefactor $2\pi l/nc$ has been dropped and the higher-order (p^2) term has been neglected. As the linear absorption of the probe pulse does not depend on the delay time Δt, the definition (5) is, up to an additive constant, equivalent to the experimentally detected signal, which is the difference between the probe transmission with and without preparation of the sample by the pump pulse. Equation (5) can also be derived by integrating the classical electrodynamical field-energy rate $E(t)(\partial/\partial t)P(t)$ [43], implying that the IPP signal is proportional to the total energy that is gained or dissipated by the probe field.

As can be seen directly from Eq. (5), the duration of measurement is determined by the probe-pulse duration, i.e., in the limit of ultrashort pulses we perform a true real-time measurement of the system dynamics. The resolution of the IPP signal with respect to the probe carrier frequency ω_2 is therefore limited by the probe-pulse duration.

In order to obtain the spectrum of the emitted field (4), one has to disperse the probe pulse with a spectrometer after it has passed the sample. As the PP signal is usually measured as the time-integrated energy rate [cf. Eq. (5)], the corresponding spectrum may be considered as stationary although it inherently depends on the delay time Δt. In this case the effect of the spectrometer [45] need not be considered in the theoretical description [40].

We define the dispersed pump-probe (DPP) signal as the difference between the intensity of the Fourier transform of the total emitted field (4) and the intensity of the Fourier transform of the incident field (3), yielding

$$\begin{aligned}I(\omega,\Delta t)&=|E_2(l,\omega)|^2-|E_2(\omega)|^2\\&=2\omega_2\mathrm{Im}E_2(\omega)P^{(3)*}(\omega)\ ,\end{aligned} \tag{6}$$

where

$$E_2(\omega)=\int_{-\infty}^{\infty}dt\,e^{i\omega t}\varepsilon_2(t)e^{-i\omega_2 t}\ , \tag{7}$$

$$P^{(3)}(\omega)=\int_{-\infty}^{\infty}dt\,e^{i\omega t}p^{(3)}(t)e^{-i\omega_2 t} \tag{8}$$

are the Fourier transforms of the incident field and the polarization, respectively. Higher-order terms and some prefactors have again been dropped. The IPP signal (5) is related to the DPP signal (6) by integration over all emission frequencies

$$I(\Delta t)=2\,\mathrm{Im}\,\omega_2\int_{-\infty}^{\infty}\frac{d\omega}{2\pi}E_2(\omega)P^{(3)*}(\omega)\ . \tag{9}$$

The DPP signal is often alternatively defined as the transmission spectrum normalized to the spectrum of the incident field [6,10,23–25], which makes it possible in the limit of an optically thin medium to express the transmission spectrum in terms of an exponential law [5]

$$|E_2(l,\omega)|^2=|E_2(\omega)|^2e^{-\Gamma(\omega,\Delta t)l}\ , \tag{10}$$

$$\Gamma(\omega,\Delta t)=\frac{4\pi\omega_2}{nc}\mathrm{Im}P^{(3)}(\omega)/E_2(\omega)\ . \tag{11}$$

Assuming the probe-pulse spectrum $E_2(\omega)$ to be known, the information on the system dynamics gained by a DPP experiment is contained in the spectrum of the probe-induced polarization. According to Eq. (8) the frequency resolution of $P^{(3)}(\omega)$ is determined by the lifetime of the polarization, which decays on the time scale of the coherence dephasing time T_2 in the case of a two-level system [43]. This results in a homogeneous linewidth of the DPP spectrum of $\hbar/T_2$.

It should be noted that an interpretation of the DPP signal defined by (11) in terms of a transient absorption spectrum may be misleading. By definition, absorption can only occur during the presence of the pulse in the sample. The frequency resolution of a transient absorption spectrum is thus determined by the field-sample interaction time, which vanishes for ultrashort pulses in optically thin samples. It follows from Eqs. (6) and (8) that the relevant time scale for the measurement is rather the decay time of the electronic polarization. It is therefore possible to achieve simultaneously high resolution in both time and frequency domain. The DPP signal, however, does not represent a true real-time measurement, in the sense that an observable of the material system is detected at a specific time, even when ultrashort pulses are employed. This fact is nicely demonstrated in recent experiments on semiconductors [46] and dyes [6], where the DPP spectrum has been recorded also for negative delay times Δt, i.e., for probe pulses arriving before the pump pulse. It has been found that long *before* zero delay a rise of the signal occurs, accompanied by strong spectral oscillations, which obviously cannot be related to the real-time dynamics of the medium induced by the pump pulses. This phenomenon arises because the presence of the pump field modifies the otherwise free induction decay of the probe-induced polarization. This effect disappears when one integrates the DPP spectrum.

III. IMPULSIVE LIMIT

The interpretation of real-time PP spectra is complicated by the fact that the observed signals in general depend on the properties of the laser pulses (e.g., carrier frequency and pulse duration) as well as on the molecular dynamics. It is therefore most helpful to consider idealized limiting cases, where the measured signals, at least in principle, become independent of the details of the experimental setup. Classic cw spectroscopy corresponds to the limiting case of stationary laser fields, which implies in practice that the duration of the measurement has to be much longer than the time scale of the system dynamics under consideration. In order to establish an analogous simple limiting case for time-resolved PP spectroscopy, one has to meet the complementary condition, that is, the duration of measurement has to be short compared to the system dynamics under consideration.

The assumption of infinitely short pulses (δ-function pulses) is quite natural for the theoretical description of time-resolved spectroscopy and has been introduced by several authors [21–28]. However, δ-function pulses are neither available nor actually desired (they would simultaneously excite *all* dipole-allowed electronic states of the system). It is therefore appropriate to define the limiting case of ultrashort pulses, henceforth referred to as the impulsive limit, more precisely.

Let us characterize the molecular system by two time scales, namely, the period corresponding to the electronic excitation energy Δ ($\hbar/\Delta\approx 1$ fs) and the period of a typical vibrational motion with frequency ω_v ($\hbar/\omega_v\approx 100$ fs). The impulsive limit is realized if (i) the laser frequencies are approximately resonant with the electronic transition ($\omega_1\simeq\omega_2\simeq\Delta$) and (ii) the pulse duration is long compared to $\hbar/\Delta$ but short compared to the vibrational period $\hbar/\omega_v$. Note that a laser pulse meeting these conditions coherently excites all vibrational levels of a given excited electronic state according to the Condon principle. A central goal of this paper is to clarify which time-dependent observables of the molecular system are reflected in the impulsive limit by the IPP and DPP signals, respectively.

Let us assume that a dipole-allowed excited electronic state, for example, a higher singlet state in a closed-shell system, is populated at $t=0$ by excitation from the ground state with an ultrashort laser pulse, such that all Condon-accessible vibrational states are coherently excited. The thus prepared non-stationary state represents a coherent wave packet, which evolves on the excited-state potential-energy surface. Excluding for the present discussion dissociative or photochemical isomerization processes, the wave packet may decay by intramolecular non-Born-Oppenheimer coupling with lower-lying electronic states (internal conversion and intersystem crossing). In many cases, at least in fairly symmetric polyatomic systems, these lower excited states will be dark in absorption, that is, they will possess vanishing transition dipole moments with the electronic ground state. When probing the time-dependent dynamics at the delay time Δt by an ultrashort pulse, only the remaining population of the bright electronic state can then contribute to the stimulated emission. It is easy to show that the IPP signal in the impulsive limit is given by [21]

$$I(\Delta t)\sim P_e(\Delta t)$$

with

$$P_e(t)=\langle\Psi(t)|\varphi_e\rangle\langle\varphi_e|\Psi(t)\rangle\ . \tag{12}$$

Here $|\Psi(t)\rangle$ is the nonstationary molecular state vector and $P_e(t)$ is the time-dependent total *electronic population* probability of the dipole-allowed diabatic state $|\varphi_e\rangle$. $P_e(t)$ is a purely intramolecular observable, independent of laser-field properties. By its definition as an electronic *population*, $P_e(t)$ is not affected by electronic pure dephasing processes [41]. It is thus a conveniently detectable observable even in complex systems, where electronic dephasing times are generally very short, typically of the order of 10 fs. It is also seen that the impulsive IPP signal is independent of the probe carrier frequency ω_2. In the absence of vibronic coupling of $|\varphi_e\rangle$ with other electronic states, $I(\Delta t)$ becomes, moreover, independent of the delay time Δt. The IPP signal (5) in the impulsive limit thus emerges as a particularly useful tool to detect directly non-Born-Oppenheimer electronic population dynamics in excited electronic states, without interference from effects of vibrational motion and electronic dephasing.

A beautiful example for the real-time observation of electronic population dynamics is provided by the experiments of Zewail and collaborators on sodium iodide [13], where excited-state absorption with fluorescence detection has been employed as probing mechanism. Given an excited-state vibrational period of $\simeq 1.25$ ps and a probe-pulse duration of 50 fs, the impulsive limit is not fully realized in this experiment [13]. The observed oscillations [13] arise from the combined effect of electronic population dynamics and vibrational wave-packet motion. A detailed theoretical analysis of this relatively transparent case has been given in Refs. [18,26,36,38,47–52].

Let us next consider the DPP spectrum as defined in Eq. (6). In the impulsive limit the pulse spectrum $E_2(\omega)$ is approximately constant over the absorption band of the electronic transition under consideration. In the impulsive limit the DPP signal is thus essentially given by the spectrum $P^{(3)}(\omega)$ of the probe-induced polarization.

As has been discussed by several authors, the spectral decomposition of the emission signal yields information about the vibrational dynamics on the excited electronic potential-energy surface [6,10,25,36]. In a classical picture the instantaneous emission frequency is given by the vertical energy gap between the two electronic surfaces at the position of the wave packet. The center of the emission spectrum is therefore correlated with the motion of the wave packet on the excited electronic potential-energy surface. As desired, the resulting time- and frequency-resolved DPP spectrum depends solely on dynamical properties of the molecular system. The homogeneous linewidth of the DPP spectrum is given by the coherence decay rate, and the time dependence of the signal is determined by the dynamical response of the system [23–25].

In recent work Pollard *et al.* have analyzed the DPP spectrum for the case of wave-packet dynamics on a single one-dimensional excited-state potential-energy surface [25]. It has been shown that the effect of coherent vibrational motion remains observable in the impulsive limit in contrast to the IPP signal, as discussed above.

In the present work we have evaluated the DPP signal (6) for a model system with non-Born-Oppenheimer coupling in the excited electronic states (see Sec. V). As expected according to the above discussion, the DPP signal reflects both electronic population dynamics, the effects of vibrational motion and vibrational dephasing, as well as electronic dephasing of the optical transition. The interpretation of the time- and frequency-resolved DPP signal is thus considerably more involved than the interpretation of the IPP signal in the impulsive limit. In practice, it will generally be difficult to separate the effects of electronic population dynamics and vibrational dynamics in the time- and frequency-resolved DPP spectrum. It is therefore of interest to know that frequency integration of the DPP spectrum in the impulsive limit eliminates the effects of vibrational motion as well as electronic dephasing, and thus exhibits the pure electronic population dynamics.

IV. EFFECTS OF FINITE-PULSE DURATION

Having seen how the integrated and dispersed impulsive PP signals can be directly interpreted in terms of vibrational and electronic dynamics, it is essential to discuss the effects of finite-pulse duration in order to see whether the real-time information remains observable with experimentally realizable pulses. In the following we restrict ourselves to the discussion of the effects of finite *probe* pulses. It has been shown elsewhere that in the case of resonant excitation the stimulated-emission signal is less sensitive to the pump-pulse duration than to the probe-pulse duration [41]. Furthermore, we want to focus on the case of nonoverlapping pump and probe pulses. As is well known, the PP signal for overlapping pulses depends on the coherence properties of the laser fields (so-called coherent artifacts) [53]. These effects are not of interest when investigating the material system dynamics.

In the impulsive limit the pulse duration is short compared to the vibrational period, with the consequence that (i) the time dependence of the signal is solely determined by the molecular dynamics, and (ii) the frequency spectra of the pump and probe pulses cover a significant part of the absorption and the emission band, respectively. For finite pulses these two conditions have to be relaxed, i.e., only a part of the absorption and emission band is excited or stimulated and the time resolution is eventually limited by the pulse duration. The polarization $P(t,\Delta t)$, induced by a finite probe pulse $E_2(t)$ centered at the delay time Δt, can be simply expressed through the corresponding polarization $P^{\delta}(t,\Delta t)$ in the impulsive limit via

$$P(t,\Delta t)=\int_{-\infty}^{t} dt' E_2(t')P^{\delta}(t,t') \ . \tag{13}$$

Inserting (13) into Eqs. (6) and (8), the DPP spectrum for finite probe pulses can be written as [25]

$$I(\omega,\Delta t)=2\omega_2 \mathrm{Im} E_2(\omega)\int_{-\infty}^{\infty} dt\, E_2(t)P^{\delta}(\omega,t) \ , \tag{14}$$

where $P^{\delta}(\omega,\Delta t)$ is the Fourier transform of $P^{\delta}(t,\Delta t)$ with respect to t, the imaginary part of it being proportional to the DPP spectrum in the impulsive limit.

Equation (14) elucidates the effects of the finite duration of the probe pulse on the DPP spectrum. Owing to the integration in (14) the time resolution is determined by the probe duration, while the spectral width of the probe pulse defines the "frequency window" of the observed emission spectrum. As discussed in Sec. II, the frequency resolution of the DPP spectrum, however, is not affected by the probe-pulse duration.

Let us consider, for the sake of illustration, a Gaussian probe pulse of duration [full width at half maximum (FWHM)] $\tau_2=20$ fs with a corresponding spectral width of 1500 cm^{-1}, which is sufficiently short to resolve a typical vibrational period. Due to intramolecular or solvent-induced relaxation processes, however, the emission spectrum may be redshifted by several thousand wave numbers with respect to the absorption spectrum. For a system with a strongly redshifted spectrum only a fraction of the emission band can therefore be stimulated with 20-fs pulses. With increasing probe-pulse duration the probe carrier frequency thus becomes an essential parameter.

Combining Eqs. (9) and (14) we can also understand the dependence of the integrated PP signal on the duration of the probe pulse. In contrast to the IPP signal in the impulsive limit, which is independent of the probe carrier frequency by definition, it is possible to measure a frequency-dependent IPP spectrum with a probe pulse of finite duration. Qualitatively, the maximum of the frequency distribution of the IPP spectrum reflects the instantaneous vertical energy gap between the radiatively coupled electronic surfaces. The IPP spectrum taken with suitable finite pulses therefore allows for the real-time observation of the vibrational motion on the excited electronic surfaces (see Refs. [4,9] for experimental observations of this effect). As has been discussed in Sec. II, the frequency resolution of the IPP spectrum is Fourier limited with respect to the probe-pulse duration, in contrast to the frequency resolution of the DPP spectrum, which is determined by the polarization decay time in the limit of short pulses.

V. MODEL APPLICATION: ULTRAFAST S_2-S_1 INTERNAL CONVERSION IN PYRAZINE

In order to illustrate and substantiate the statements of Secs. III and IV, we present some results of a computational study of femtosecond PP signals for a suitable model of ultrafast intramolecular dynamics. In contrast to other recent studies of the fundamentals of molecular femtosecond real-time spectroscopy, which have assumed either one-dimensional shifted-harmonic-oscillator models with phenomenological electronic dephasing for the excited-state dynamics [22–30,40] or phenomenological Brownian-oscillator models [27,31], our model for the material system represents multidimensional vibrational motion with strong non-Born-Oppenheimer coupling between two excited electronic potential-energy surfaces. As discussed in detail elsewhere [41,42], the model has been devised to rationalize the ultrafast internal conversion process in the second excited singlet $(\pi\pi^*)$ state of pyrazine in terms of a conical intersection with the first excited singlet $(n\pi^*)$ state. The vibronic dynamics is treated microscopically by solving the time-dependent Schrödinger equation, taking account of three nonseparable vibrational degrees of freedom. It has been shown that the model accounts for ultrafast non-Markovian electronic population decay and electronic dephasing, as well as rapid dephasing of coherent vibrational motion in the S_2 state [42]. Additional relaxation effects in the excited-state manifold (pure electronic dephasing owing to fluctuations in the remaining vibrational models as well as population decay into the electronic ground state) are taken into account via phenomenological electronic dephasing ($T_2=30$ fs) and decay ($T_1=500$ fs) constants [54].

For the present purposes we adopt this system as a nontrivial model of ultrafast excited-state relaxation, for which we wish to investigate the possibility of time- and frequency-resolved PP spectroscopy. Applying time-dependent density-matrix perturbation theory with respect to the field-matter interaction, the nonlinear polarization $p^{(3)}(t)$ entering in Eqs. (5) and (8) is calculated [41]. We have neglected in this calculation the contributions which correspond to stimulated impulsive Raman processes [28–31]. These contributions vanish in the limit of ultrashort pulses and are not of relevance in the present context.

Let us first consider the PP signals in the impulsive limit. As has been discussed above, the IPP signal in the ideal impulsive limit is independent of the probe carrier frequency and purely a function of the pulse delay time.

Figure 1 shows the IPP signal of the model in the impulsive limit as a function of the delay time Δt. As discussed above [Eq. (12)], the impulsive IPP signal monitors the total time-dependent population probability $P_e(t)$ of the optically excited electronic state. On the time scale of Fig. 1 (600 fs), the phenomenological population decay represented by $T_1=500$ fs is of little relevance. The oscillatory decay of the signal in Fig. 1 rather reflects the nonadiabatic electronic dynamics of the S_2 state owing to

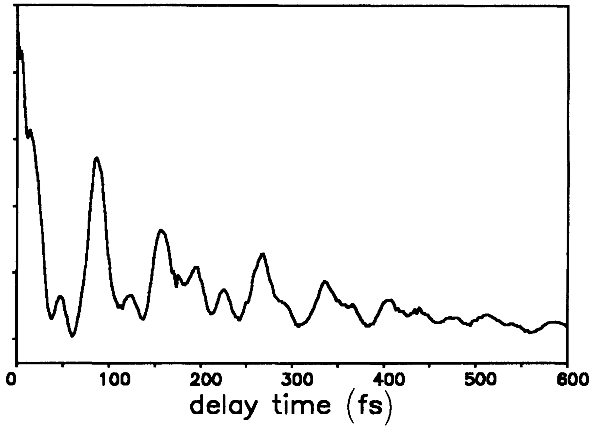

FIG. 1. Integrated PP signal in the impulsive limit for the three-state three-mode model system of pyrazine (see text) as a function of the pulse delay time. The signal reflects the population dynamics of the optically excited $S_2(\pi\pi^*)$ electronic state, caused by the vibronic coupling with the $S_1(n\pi^*)$ state.

vibronic coupling with the lower-lying S_1 state. It is seen that the short-time electronic decay dynamics is strongly non-Markovian. It should also be stressed that the electronic population probability $P_e(t)$ shown in Fig. 1 cannot be recovered by Fourier transformation from the cw absorption spectrum (see Refs. [21,41] for a detailed discussion). The impulsive IPP signal therefore yields novel information on the electronic excited-state dynamics.

Figure 2 shows the time- and frequency-resolved impulsive DPP spectrum for the S_1-S_2 vibronic coupling model of pyrazine (evaluated with δ-function pulses). For zero delay time the emission spectrum is equivalent to the stationary absorption spectrum of the S_2 state. The decay of the signal as a function of time qualitatively reflects the electronic population dynamics. The frequency distribution of the signal, on the other hand, reflects the evolution of the vibrational character of the system. It is seen that within $\Delta t \approx 20$ fs the DPP spectrum undergoes a dramatic redshift, which reflects the change of the vibrational character of the wave function during the ultrafast initial $S_2 \rightarrow S_1$ decay. For larger Δt the stimulated-emission signal remains redshifted ($\Delta\omega \simeq 1.2 \times 10^4$ cm^{-1}). The redshift of the emission signal reflects the conversion from initially prepared S_2 levels into high vibrational levels of the S_1 surface, from which, according to the Condon principle, emission can be stimulated only to correspondingly high levels of S_0.

In the absence of vibronic coupling of the optically prepared S_2 state with the lower-lying S_1 state, the centroid of the DPP spectrum would shift periodically with time, reflecting coherent vibrational motion in the S_2 state (see Ref. [25] for a one-dimensional example). The absence of this simple periodic motion in Fig. 2 reflects the strong perturbation of the excited-state dynamics by the conical intersection of the potential-energy surfaces, which results in a dephasing of the initially coherent vibrational motion on femtosecond time scales [42] (not to be confused with the dephasing of the S_0-S_2 electronic coherence). It should be stressed that the time dependence of the DPP signal in Fig. 2 is not significantly affected by the phenomenological electronic dephasing time. The parameter T_2 simply determines the resolution of the DPP signal with respect to frequency. If T_2 were longer, the signal in Fig. 2 would show sharper structures as a function of frequency, but the overall shape of the signal would remain unchanged.

It can be summarized that the DPP signal, if arbitrarily short probe pulses were available, would yield very detailed information on the dynamics in excited electronic states. In the example considered here, which involves multimode vibronic coupling of two excited electronic states, the impulsive DPP signal monitors the time evolution of the electronic as well as the vibrational character of the excited-state wave function. The frequency resolution of the signal is determined by the polarization decay time; the detectability of the electronic population dynamics and the vibrational dynamics is not limited, how-

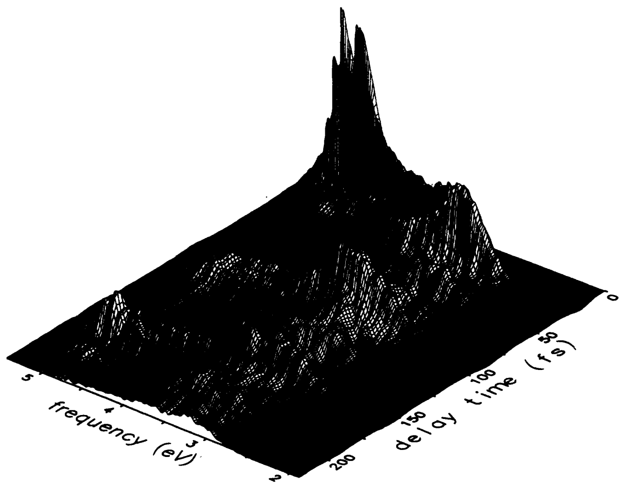

FIG. 2. Dispersed PP spectrum in the impulsive limit for the three-state three-mode model of pyrazine, as a function of delay time and frequency setting of the spectrometer.

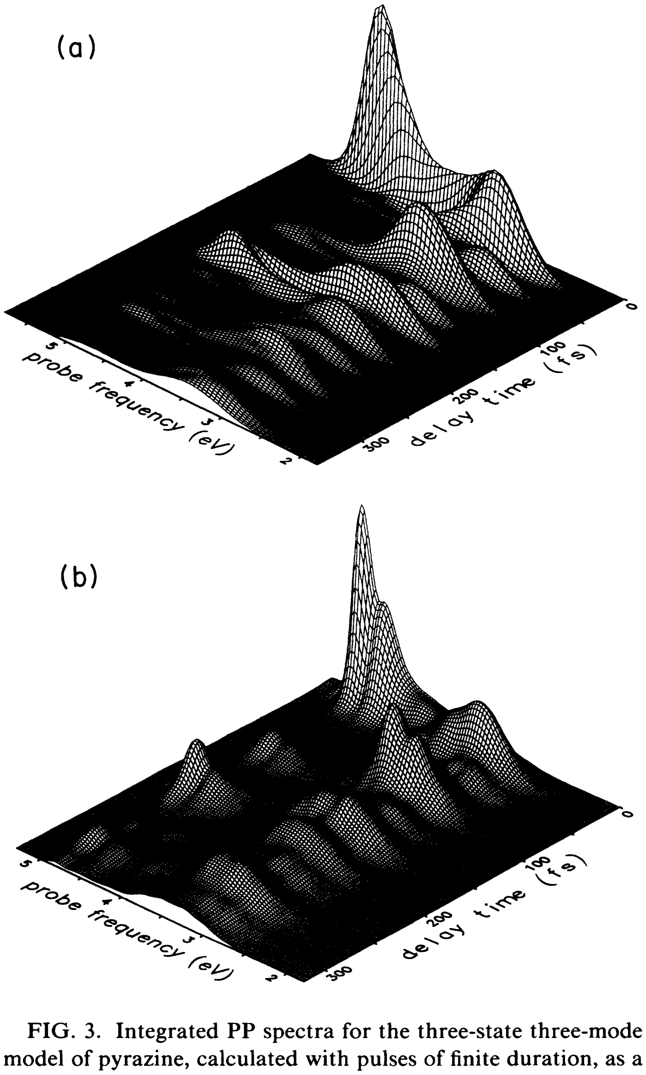

FIG. 3. Integrated PP spectra for the three-state three-mode model of pyrazine, calculated with pulses of finite duration, as a function of delay time and carrier frequency of the probe pulse. (a) pump- and probe-pulse duration 6 fs; (b) pump- and probe-pulse duration 20 fs.

ever, by the time scale of the electronic polarization decay.

Let us now consider PP spectra obtained with pulses of finite duration for the model system. In the case of the IPP spectrum we gain frequency resolution while losing time resolution with increasing probe-pulse duration. As an illustration, Figs. 3(a) and 3(b) show the IPP signal for the model as a function of both delay time and probe carrier frequency ω_2 for pulses of 6 and 20 fs duration, respectively. The frequency of the pump pulse is resonant to the center of the S_2 absorption band. For such short pulses, the frequency resolution is determined by the pulse duration, and the signal becomes strictly independent of the phenomenological electronic dephasing time T_2. It is seen that the IPP measurement with finite pulses allows the real-time detection of both the electronic character (via the intensity of the signal) as well as the vibrational character (via the frequency distribution of the signal) of the excited-state wave function. It is also seen that the impulsive DPP signal in Fig. 2 and the IPP signal in Fig. 3 provide largely equivalent pictures of the excited-state dynamics. It should be kept in mind, however, that the signal in Fig. 2 requires a δ-function probe pulse, whereas the signals in Fig. 3 are obtained with physically realizable pulses.

DPP signals obtained with pulses of finite duration are shown in Fig. 4. As discussed above [Eq. (14)], the spectral width of the probe pulse defines the accessible frequency window. Even with 6-fs pulses, only a fraction of the frequency spectrum in Fig. 2 can be covered. In order to enhance the information content, Figs. 4(a) and 4(b) contain the signals for two choices of the probe carrier frequency (ω_2=4.84 eV at the left-hand side, ω_2=3.30 eV at the right-hand side). It is seen that with 20-fs pulses only a narrow slice of the impulsive DPP signal is obtained. The information contained in the impulsive DPP spectrum (Fig. 2) can be reconstructed if the finite-pulse DPP spectrum is recorded for a sufficiently dense set of probe carrier frequencies.

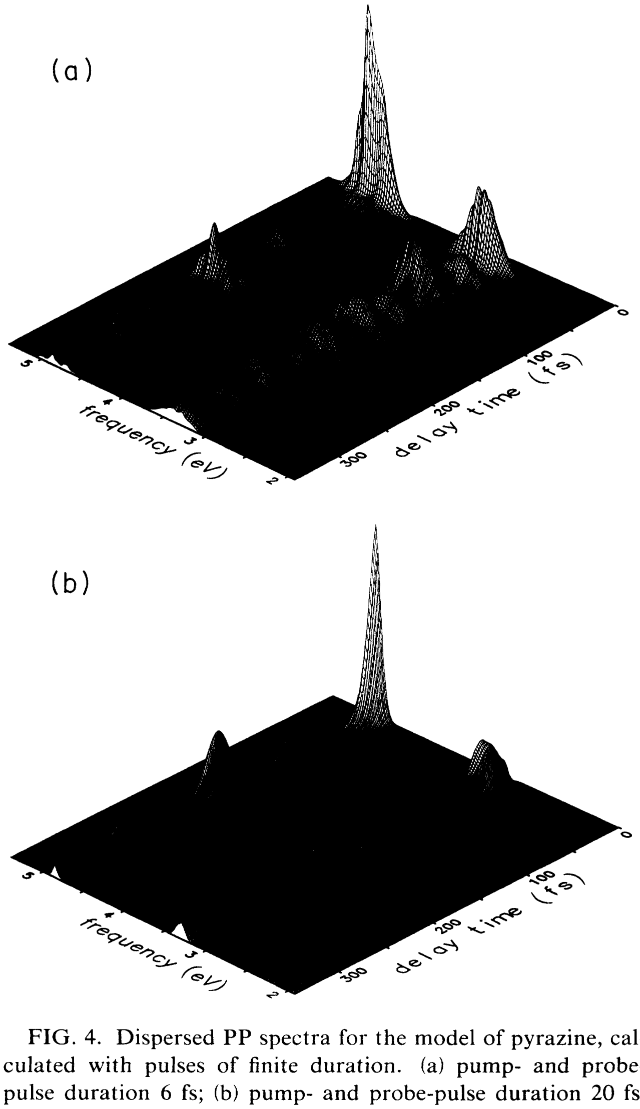

FIG. 4. Dispersed PP spectra for the model of pyrazine, calculated with pulses of finite duration. (a) pump- and probe-pulse duration 6 fs; (b) pump- and probe-pulse duration 20 fs. The signals for two probe carrier frequencies (ω_2=4.48 eV at the left-hand side, ω_2=3.30 eV at the right-hand side) are combined.

VI. CONCLUSIONS

Starting from a general theoretical description of time- and frequency-resolved stimulated-emission PP spectroscopy, we have focused the attention on the question of which time-dependent observables of the material system are monitored by the integral and the dispersed PP signals, respectively, in the limit of ultrashort pulses. The conditions for a simple and laser-pulse-independent interpretation of molecular PP signals, specifying the so-called impulsive limit, are (i) a pump pulse, which coherently excites essentially all vibrational levels of the excited electronic state according to the Condon principle, and (ii) a probe pulse, which is short enough to coherently stimulate emission into all Condon-allowed vibrational levels of the electronic ground state.

For many systems the ideal impulsive limit may not be attainable with experimentally realizable laser pulses. The analysis of this limiting case is nevertheless of interest, as it provides us with basic concepts which will prove useful for the qualitative interpretation of femtosecond real-time experiments in general.

It has been pointed out that the IPP signal has a particularly simple interpretation in the impulsive limit. The signal becomes independent of the effects of electronic dephasing as well as vibrational motion in the excited state. The delay-time dependence of the IPP signal directly reflects the population dynamics of the excited electronic state. The impulsive IPP signal thus represents a particularly transparent probe of electronic relaxation processes.

It has been demonstrated that the time- and frequency-resolved DPP signal obtained with sufficiently short pulses carries information on coherent vibrational motion (and thus also vibrational dephasing on the excited electronic surface) in addition to electronic population dynamics. As is well known, the frequency resolution of the impulsive DPP spectrum reflects directly the dephasing time of the electronic transition [6,25].

Deviations from the ideal impulsive limit owing to finite duration of the probe pulse have been discussed. For finite pulse duration, the IPP signal becomes dependent on the center frequency of the probe pulse. It thus carries additional information, which reflects the effect of coherent vibrational motion in the excited state. In the DPP spectrum, on the other hand, one loses information when a Fourier-limited probe pulse of finite duration and fixed carrier frequency is employed, owing to the finite frequency window given by the spectrum of the probe pulse. In practice, the simultaneous measurement of the IPP and DPP signals should be most helpful for the disentangling of the complex electronic and vibrational dynamics in short-lived excited states of polyatomic molecules. It should once more be stressed that this real-time information cannot be simply extracted, via Fourier transformation, from the conventional cw absorption spectrum [21,41].

When considering time- and frequency-resolved femtosecond spectroscopy, the question naturally arises whether the well-known time-frequency uncertainty principle can be outwitted. In the case of the IPP signal we have seen that the duration of the measurement is given by the temporal width of the probe pulse. Time and frequency resolution are thus Fourier limited. With infinitely short pulses, in particular, any frequency resolution is lost. The DPP signal, on the other hand, exhibits time *and* frequency resolution even for arbitrarily short pulses. At first glance, it seems that the time-frequency Fourier limitation has been overcome. However, the duration of the measurement in the DPP case is given by the polarization decay time, which is independent of the pulse duration. When the polarization decay time is long compared to the probe-pulse duration, the DPP signal thus does not represent a true real-time measurement in the sense that an intramolecular observable (such as the position of a wave packet) is detected at a specific time (the delay time Δt).

ACKNOWLEDGMENTS

The authors would like to thank Matthias Seel for stimulating discussions. Support by the Deutsche Forschungsgemeinschaft and the Fonds der Chemischen Industrie is gratefully acknowledged.

---

[1] C. V. Shank, in *Ultrashort Laser Pulses and Applications,* edited by W. Kaiser (Springer-Verlag, Berlin, 1988), p. 5.

[2] See papers in *Ultrashort Phenomena VII,* edited by C. B. Harris, E. P. Ippen, G. A. Mourou, and A. H. Zewail (Springer-Verlag, Berlin, 1990), Part XII.

[3] Reference [2], Part XIII.

[4] M. J. Rosker, F. W. Wise, and C. L. Tang, Phys. Rev. Lett. **57**, 321 (1986); F. W. Wise, M. J. Rosker, and C. L. Tang, J. Chem. Phys. **86**, 2827 (1987).

[5] J. Chesnoy and A. Mokhtari, Phys. Rev. A **38**, 3566 (1988); A. Mokhtari, A. Chebira, and J. Chesnoy, J. Opt. Soc. Am. B **7**, 1551 (1990).

[6] C. H. Brito Cruz, J. P. Gordon, P. C. Becker, R. L. Fork, and C. V. Shank, IEEE J. Quantum Electron. **24**, 261 (1988); H. L. Fragnito, J.-Y. Bigot, P. C. Becker, and C. V. Shank, Chem. Phys. Lett. **160**, 101 (1989).

[7] B. Fluegel, N. Peyghambarian, G. Olbright, M. Lindberg, S. W. Koch, J. Joffre, D. Hulin, A. Migus, and A. Antonetti, Phys. Rev. Lett. **59**, 2588 (1987).

[8] K. Leo, J. Shah, E. O. Göbel, T. C. Damen, S. Schmitt-Rink, W. Schäfer, and K. Köhler, Phys. Rev. Lett. **66**, 201 (1990).

[9] M. J. Rosker, M. Dantus, and A. H. Zewail, J. Chem. Phys. **89**, 6113, (1988); **89**, 6128 (1988); R. M. Bowman, M. Dantus, and A. H. Zewail, Chem. Phys. Lett. **161**, 297 (1989); M. Dantus, R. M. Bowman, M. Gruebele, and A. H. Zewail, J. Chem. Phys. **91**, 7437 (1989).

[10] J. Misewich, J. H. Glownia, J. E. Rothenberg, and P. P. Sorokin, Chem. Phys. Lett. **150**, 374 (1988); R. E. Walkup, J. A. Misewich, J. H. Glownia, and P. P. Sorokin, J. Chem. Phys. **94**, 3389 (1991).

[11] See, for example, E. P. Ippen and C. V. Shank, in *Ultrashort Light Pulses,* edited by S. Shapiro (Springer, Berlin, 1977), p. 102.

[12] M. Dantus, M. J. Rosker, and A. H. Zewail, J. Chem. Phys. **87**, 2395 (1987).

[13] M. J. Rosker, T. S. Rose, and A. H. Zewail, Chem. Phys. Lett. **146**, 175 (1988); T. S. Rose, M. J. Rosker, and A. H. Zewail, J. Chem. Phys. **91**, 7415 (1989); P. Cong, A. Mokhtari, and A. H. Zewail, Chem. Phys. Lett. **172**, 109 (1990).

[14] J. M. Wiesenfeld and B. I. Greene, Phys. Rev. Lett. **51**, 1745 (1983).

[15] T. Baumert, B. Bühler, R. Thalweiser, and G. Gerber, Phys. Rev. Lett. **64**, 733 (1990).

[16] J. M. Smith, C. Lakshminarayan, and J. L. Knee, J. Chem. Phys. **93**, 4475 (1990).

[17] M. Dantus, M. H. M. Janssen, and A. H. Zewail, Chem. Phys. Lett. **181**, 281 (1991).

[18] H. Metiu and V. Engel, J. Opt. Soc. Am. B **7**, 1709 (1990); J. Chem. Phys. **93**, 5693 (1990).

[19] M. Seel and W. Domcke, Chem. Phys. **151**, 59 (1991).

[20] V. Engel, Chem. Phys. Lett. **178**, 130 (1991).

[21] W. Domcke and H. Köppel, Chem. Phys. Lett. **140**, 133 (1987); G. Stock and W. Domcke, Chem. Phys. **124**, 227 (1988).

[22] M. Mitsunaga and C. L. Tang, Phys. Rev. A **35**, 1720 (1987).

[23] M. Lindberg and S. W. Koch, J. Opt. Soc. Am. B **5**, 140 (1988).

[24] S.-Y. Lee, W. T. Pollard, and R. A. Mathies, Chem. Phys. Lett. **160**, 531 (1989).

[25] W. T. Pollard, S.-Y. Lee, and R. A. Mathies, J. Chem. Phys. **92**, 4012 (1990); W. T. Pollard, H. L. Fragnito, J.-Y. Bigot, C. V. Shank, and R. A. Mathies, Chem. Phys. Lett. **168**, 239 (1990).

[26] B. Fain, S. H. Lin, and N. Hamer, J. Chem. Phys. **91**, 4485 (1989); S. H. Lin, B. Fain, and N. Hamer, Adv. Chem. Phys. **79**, 133 (1990).

[27] Y. J. Yan and S. Mukamel, Phys. Rev. A **41**, 6485 (1990); W. B. Bosma, Y. J. Yan, and S. Mukamel, J. Chem. Phys. **93**, 3863 (1990).

[28] I. A. Walmsley, M. Mitsunaga, and C. L. Tang, Phys. Rev. A **38**, 4681 (1988).

[29] K. A. Nelson and E. P. Ippen, Adv. Chem. Phys. **75**, 1 (1989).

[30] A. M. Walsh and R. F. Loring, Chem. Phys. Lett. **160**, 299 (1989).

[31] Y. J. Yan and S. Mukamel, J. Chem. Phys. **94**, 997 (1991).

[32] H. Kono and Y. Fujimura, J. Chem. Phys. **91**, 5960 (1989).

[33] S. H. Lin, B. Fain, and C. Y. Yeh, Phys. Rev. A **41**, 2718 (1990).

[34] P. Kowalczyk, C. Radzewicz, J. Mostowski, and I. A. Walmsley, Phys. Rev. A **42**, 5622 (1990).

[35] R. Bersohn and A. H. Zewail, Ber. Bunsenges. Phys. Chem. **92**, 373 (1988).

[36] S.-Y. Lee, W. T. Pollard, and R. A. Mathies, J. Chem. Phys. **90**, 6146 (1989).

[37] W. Strunz, G. Alber, and J. S. Briggs, J. Phys. B **23**, L697 (1990).

[38] V. Engel, H. Metiu, R. Almaida, R. A. Marcus, and A. H. Zewail, Chem. Phys. Lett. **152**, 1 (1988).

[39] S. O. Williams and D. G. Imre, J. Phys. Chem. **90**, 6636 (1988); **90**, 6648 (1988).

[40] W. Vogel, D.-G. Welsch, and B. Wilhelmi, Phys. Rev. A **37**, 3825 (1987).

[41] G. Stock, R. Schneider, and W. Domcke, J. Chem. Phys. **90**, 7184 (1989); G. Stock and W. Domcke, J. Opt. Soc. Am. B **7**, 1970 (1990).

[42] R. Schneider and W. Domcke, Chem. Phys. Lett. **150**, 235 (1988); R. Schneider, W. Domcke, and H. Köppel, J. Chem. Phys. **92**, 1045 (1990).

[43] Y. R. Shen, *The Principles of Nonlinear Optics* (Wiley, New York, 1984), Chaps. 2.1 and 3.

[44] A. Icsevgi and W. E. Lamb, Phys. Rev. **185**, 517 (1969).

[45] J. H. Eberly and K. Wódkiewicz, J. Opt. Soc. Am. **67**, 1252 (1977).

[46] M. Joffre, D. Hulin, J. P. Chambaret, A. Migus, A. Antonetti, and C. Benoit à la Guillaume, in *Ultrafast Phenomena VI,* edited by T. Yajima, K. Yashihara, C. B. Harris, and S. Shionoya (Springer-Verlag, Berlin, 1988), p. 223.

[47] S. O. Williams and D. G. Imre, J. Phys. Chem. **92**, 6636 (1988).

[48] S. H. Lin and B. Fain, Chem. Phys. Lett. **155**, 216 (1989).

[49] V. Engel and H. Metiu, J. Chem. Phys. **90**, 6116 (1989); **91**, 1596 (1989); C. Meier, V. Engel, and J. S. Briggs, *ibid.* **95**, 7337 (1991).

[50] S. E. Choi and J. C. Light, J. Chem. Phys. **90**, 2593 (1989).

[51] S. Chapman and M. S. Child, J. Phys. Chem. **95**, 578 (1991).

[52] H. Kono and Y. Fujimura, Chem. Phys. Lett. **184**, 497 (1991).

[53] H. A. Ferwerda, J. Terpstra, and D. A. Wiersma, J. Chem. Phys. **91**, 3296 (1989).

[54] G. Stock and W. Domcke, J. Chem. Phys. **93**, 5496 (1990).

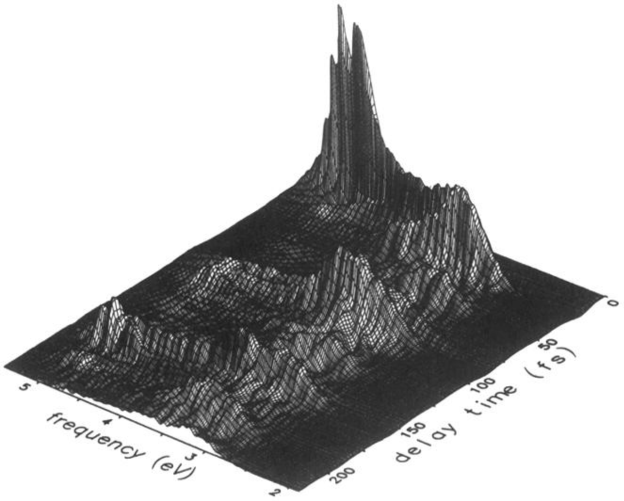

FIG. 2. Dispersed PP spectrum in the impulsive limit for the three-state three-mode model of pyrazine, as a function of delay time and frequency setting of the spectrometer.

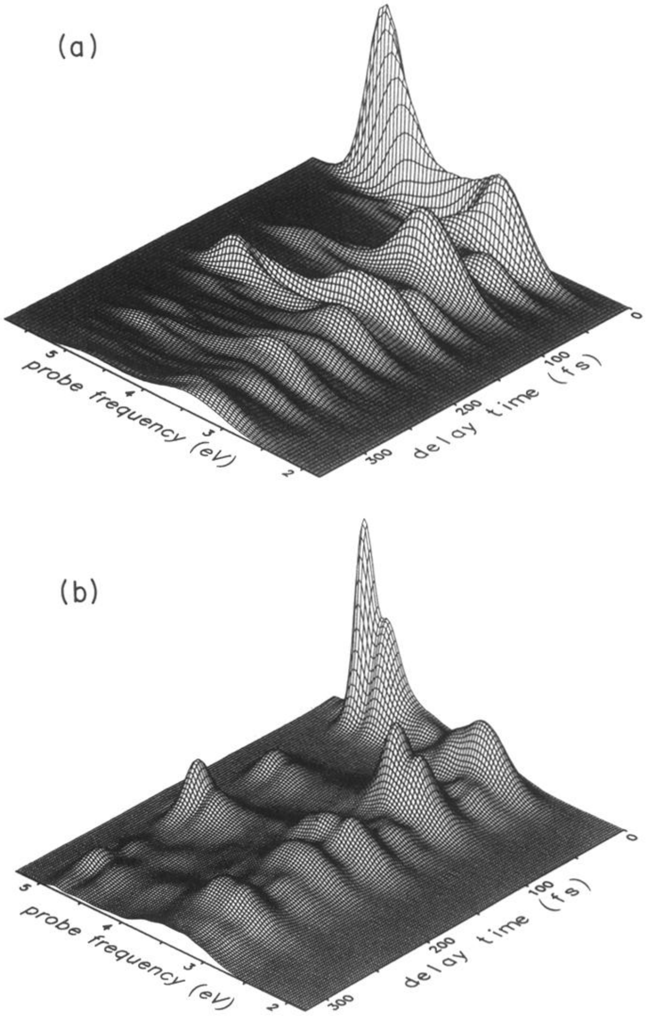

FIG. 3. Integrated PP spectra for the three-state three-mode model of pyrazine, calculated with pulses of finite duration, as a function of delay time and carrier frequency of the probe pulse. (a) pump- and probe-pulse duration 6 fs; (b) pump- and probe-pulse duration 20 fs.

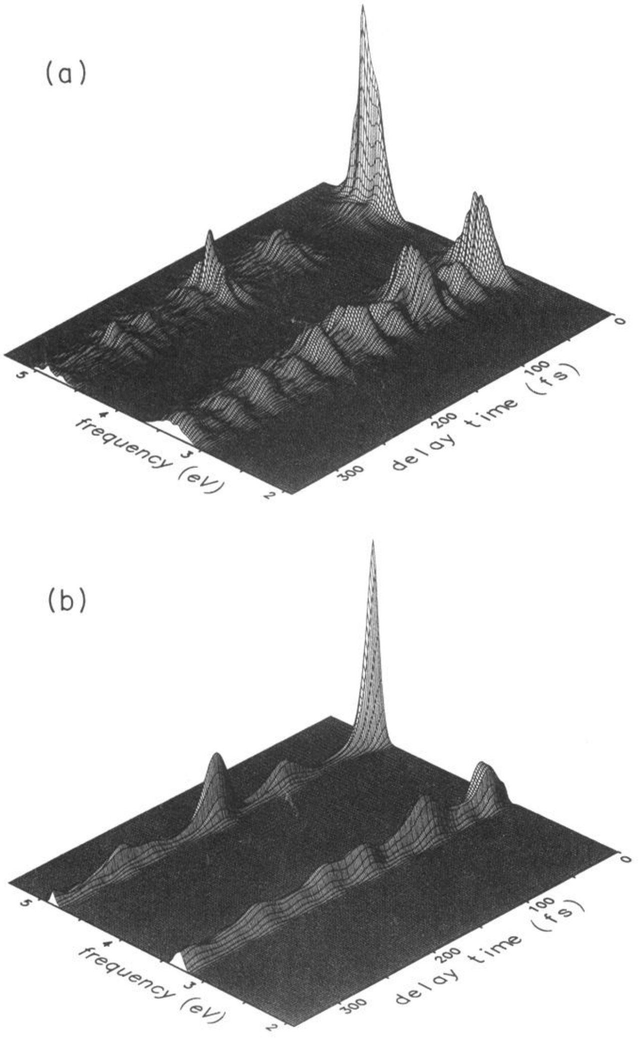

FIG. 4. Dispersed PP spectra for the model of pyrazine, calculated with pulses of finite duration. (a) pump- and probe-pulse duration 6 fs; (b) pump- and probe-pulse duration 20 fs. The signals for two probe carrier frequencies ($\omega_2 = 4.48$ eV at the left-hand side, $\omega_2 = 3.30$ eV at the right-hand side) are combined.